Electronic Supplementary Material (ESI) for Nanoscale.

Supplementary Information

Scratch to sensitize: scratch-induced sensitivity enhancement in semiconductor thin-film sensors

*Geonhee Lee, Min Choi, Soo Sang Chae, Du Won Jeong, Won Jin Choi, Seulgi Ji, Yun Ho Kim, Ji Woon Choi, Tae Il Lee, Incheol Cho, Inkyu park, Sun Sook Lee, Sungsu Park, Noejung Park, Hyunju Chang and Jeong-O Lee**

Contents

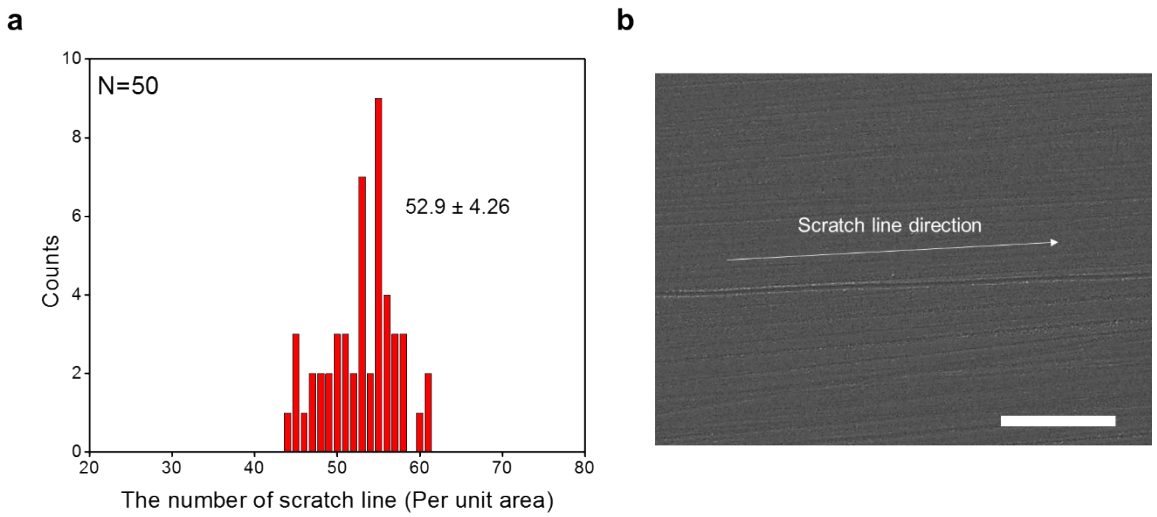

Figure S1. Statistical analysis of the number of ZnO scratch lines per unit area. SEM images were obtained at 50 points at regular intervals of 2 mm (horizontally) x 4 mm (vertically) from a 1.8 cm x 1.6 cm area of a 2 cm x 2 cm substrate. Figure S1b shows a representative SEM image of a scratched substrate. (scale bar : 1 μm) As shown in the figure, the scratch lines are fairly uniformly distributed over the ~cm scale substrate, with ~16 lines per 1 μm.

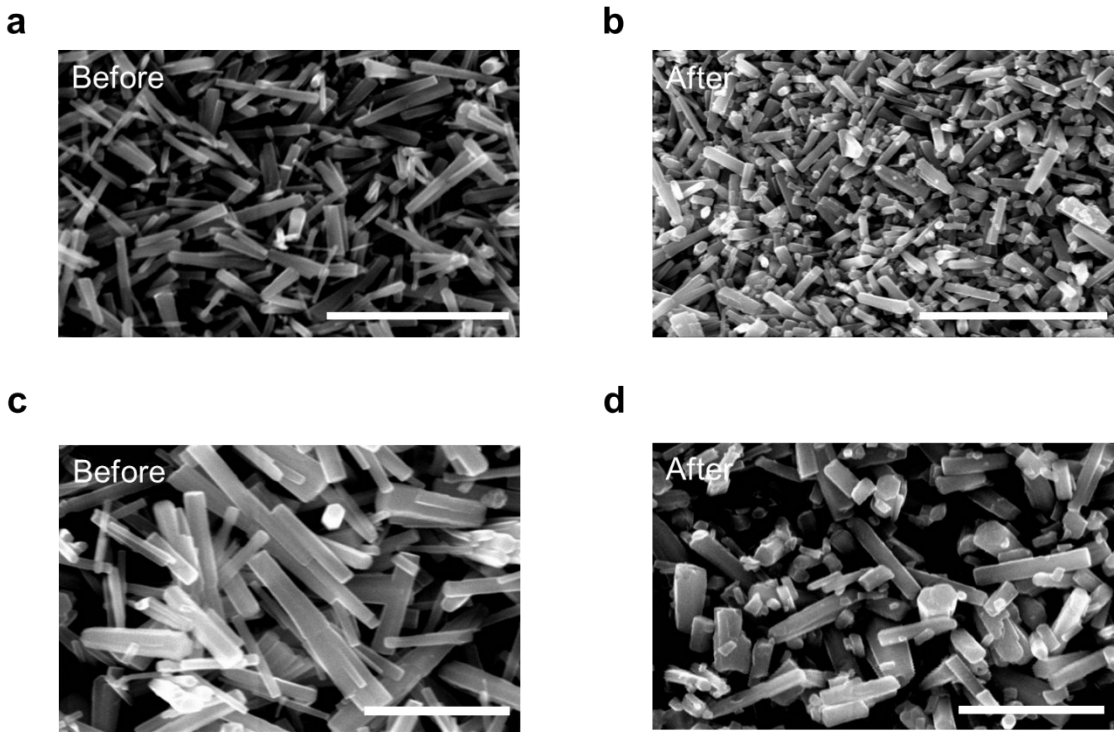

Figure S2. SEM images of ZnO powder and ground ZnO powder. (a) and (c) ZnO powder produced using the hydrothermal process.(b), (d) Ground ZnO powder made by grinding ZnO powder using a mortar. Scale bars in (a), (b) represent 5 µm and those in (c), (d) represent 2 µm.

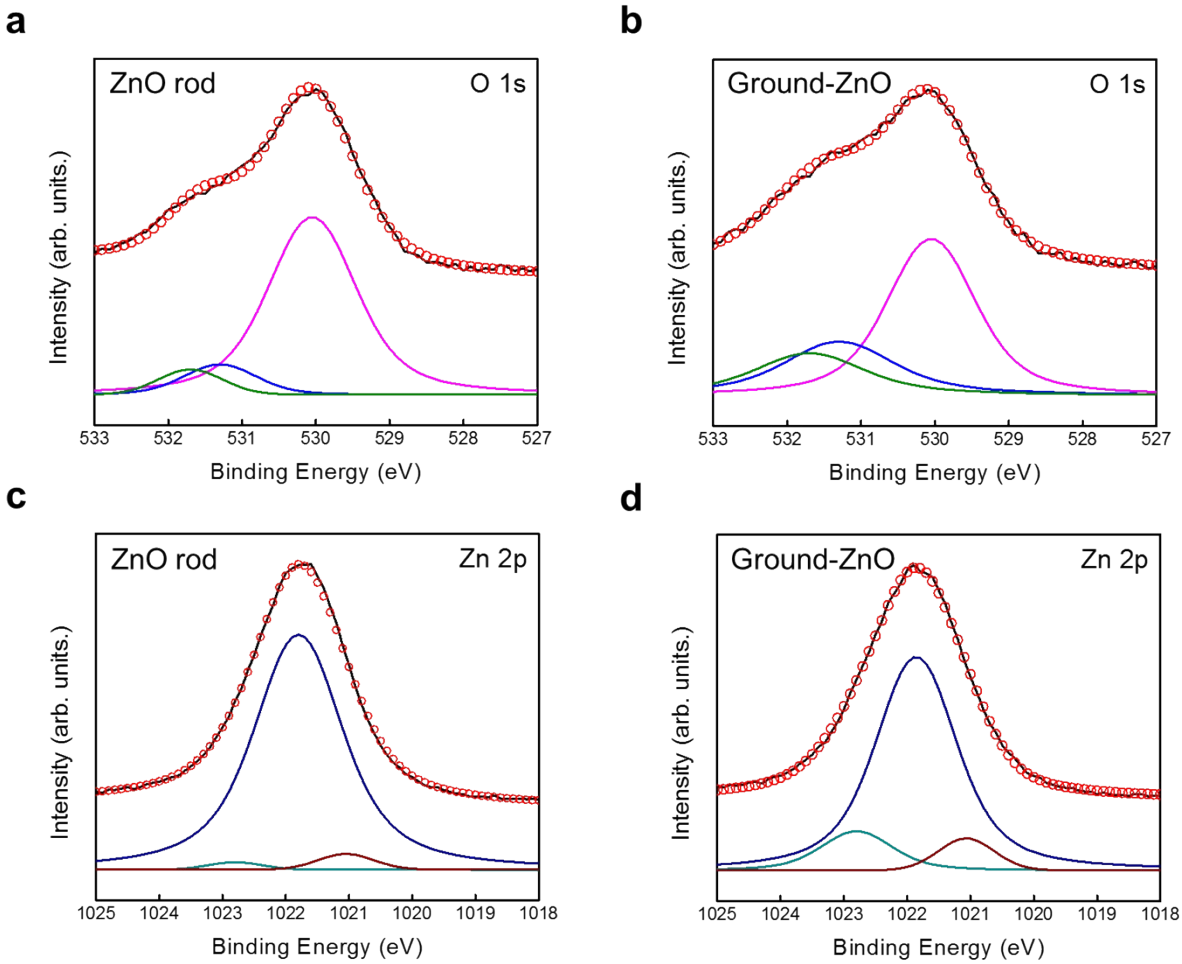

Figure S3. XPS analyses of ZnO powder and ground ZnO powder. Figures S2(a),(c) from ZnO powder and Figures S2(b),(d) from ground ZnO. O 1s peak was fitted by three peaks: those of the ZnO lattice in pink (529.9 eV), oxygen defect in green (531.4 eV), and hydroxyl groups of ZnO in blue (531.7 eV). Also, the Zn 2p peak was fitted by three peaks: those of the zinc hydroxide in dark cyan (1022.8 eV), ZnO lattice in navy (1021.7 eV), and Zn metal in wine (1021.1 eV).

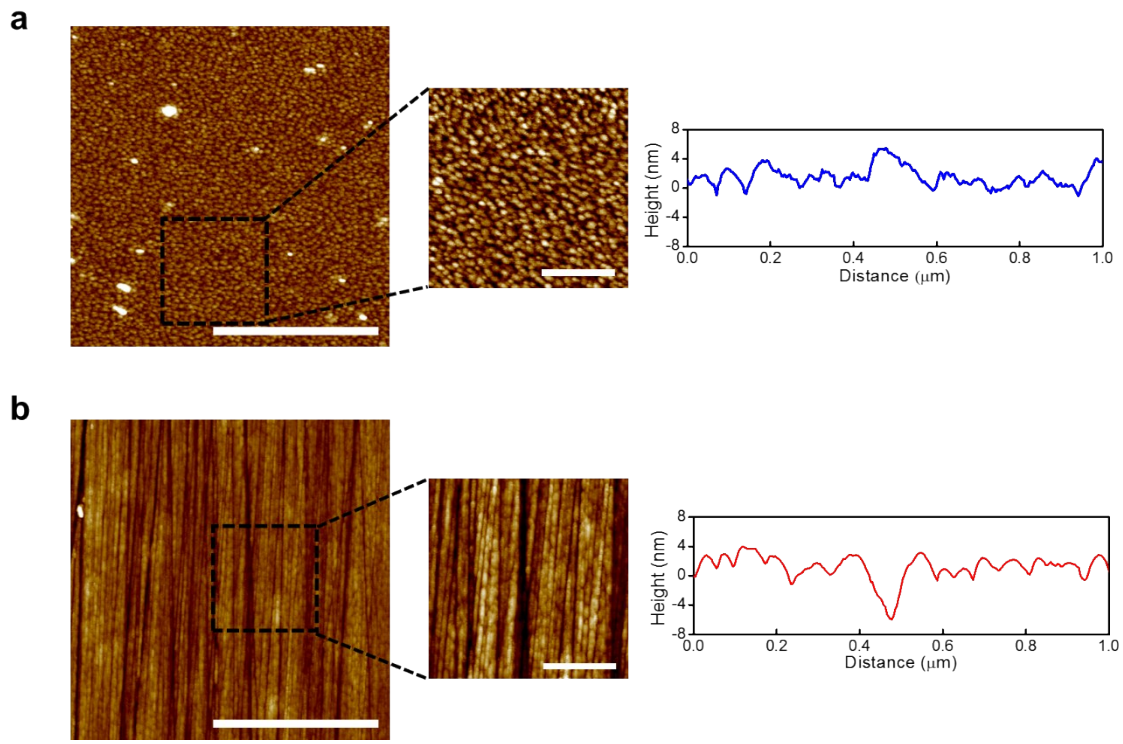

Figure S4. AFM images of sol-gel-prepared ZnO thin films (a) before and (b) after being scratched. Scale bars in the right images each represent 5 μm and those in the left images each represent 300 nm.

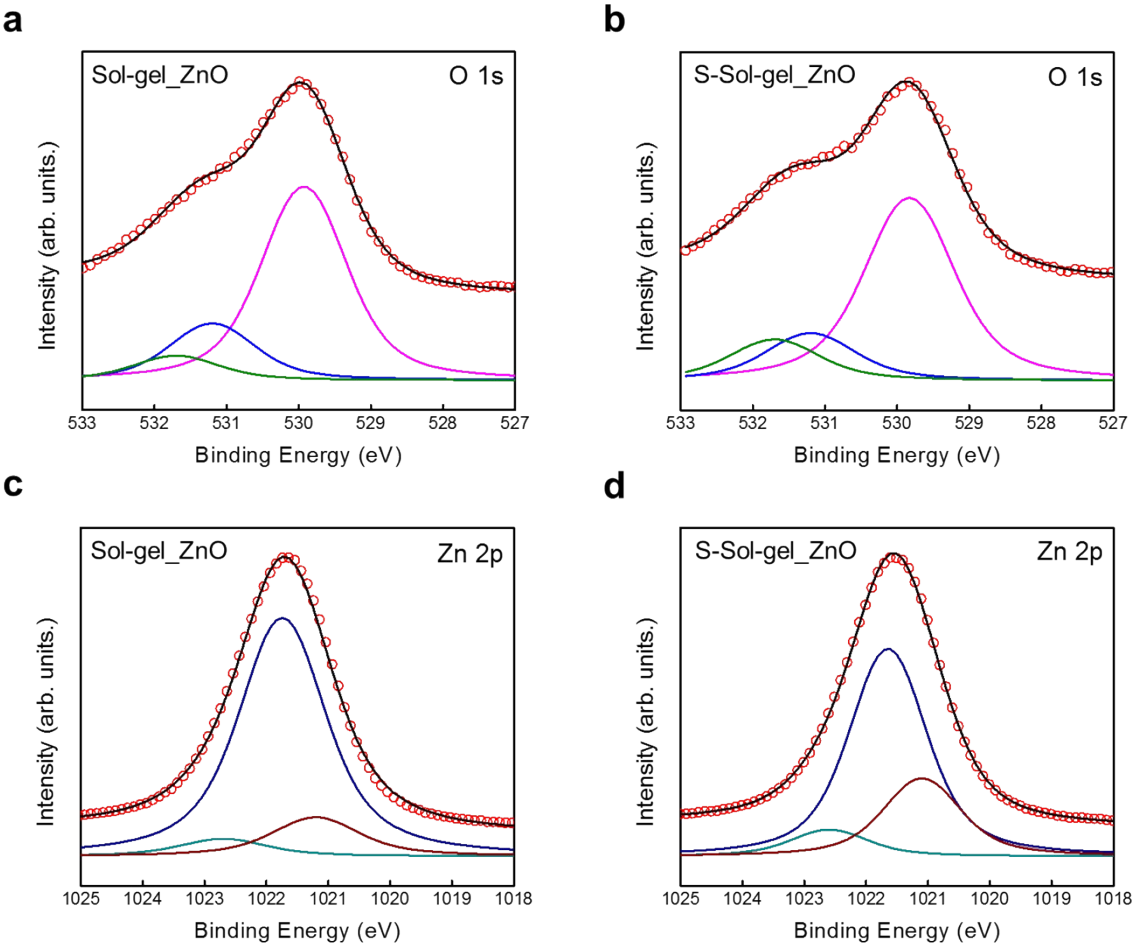

Figure S5. XPS spectra of sol-gel prepared ZnO thin films. (a), (c) before and (b), (d) after being scratched. Each O 1s peak was fitted by three peaks: those of the ZnO lattice in pink (529.9 eV), oxygen defect in green (531.4 eV), and hydroxyl groups of ZnO in blue (531.7 eV). Each Zn 2p peak was fitted by three peaks: those of zinc hydroxide in dark cyan (1022.8 eV), ZnO lattice in navy (1021.7 eV), and Zn metal in wine (1021.1 eV).

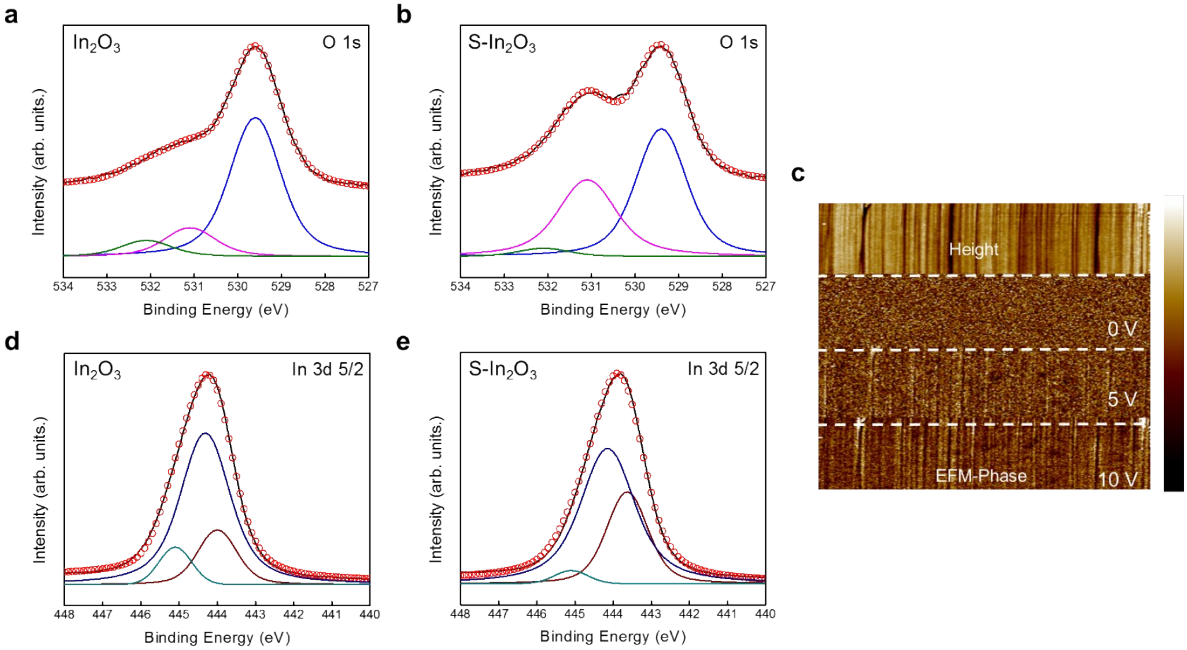

Figure S6. XPS spectra of In_2O_3 and S-In_2O_3 films. Figure S6(a),(d) from normal In_2O_3 film and Figure S6b,e from a scratched In_2O_3 film. Each O 1s peak was fitted by three peaks: those of the In_2O_3 lattice in blue (529.5 eV), oxygen defect in pink (531.1 eV), and hydroxyl groups of the In_2O_3 in green (532.3 eV). Also, each In 3d 5/2 peak was fitted by three peaks: those of In metal in dark cyan (443.7 eV), In_2O_3 lattice in navy (444.3 eV), and $In(OH)_3$ in wine (445.2 eV). (c) The AFM height and EFM-Phase image of the S-In_2O_3 region; the EFM image was obtained with varying the applied voltage at a fixed tip height of 100 nm.

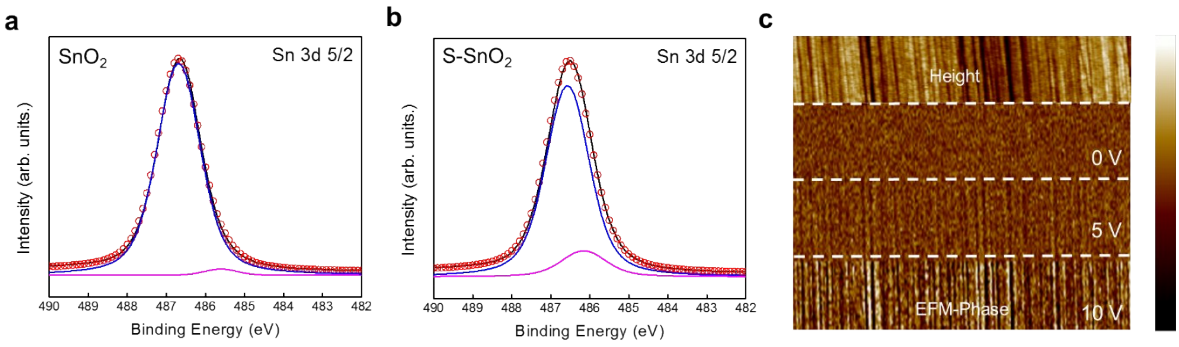

Figure S7. XPS spectra of SnO_2 and S-SnO_2 films. (a) SnO_2 film spectrum. (b) S-SnO_2 film spectrum. In 3d 5/2 peak was fitted by two peaks: those of the Sn metal in pink (486.1 eV) and SnO_2 lattice in blue (486.6 eV). (c) The AFM height and EFM-Phase image of the S-SnO_2; the EFM image was obtained with varying the applied voltage at a fixed tip height of 100 nm.

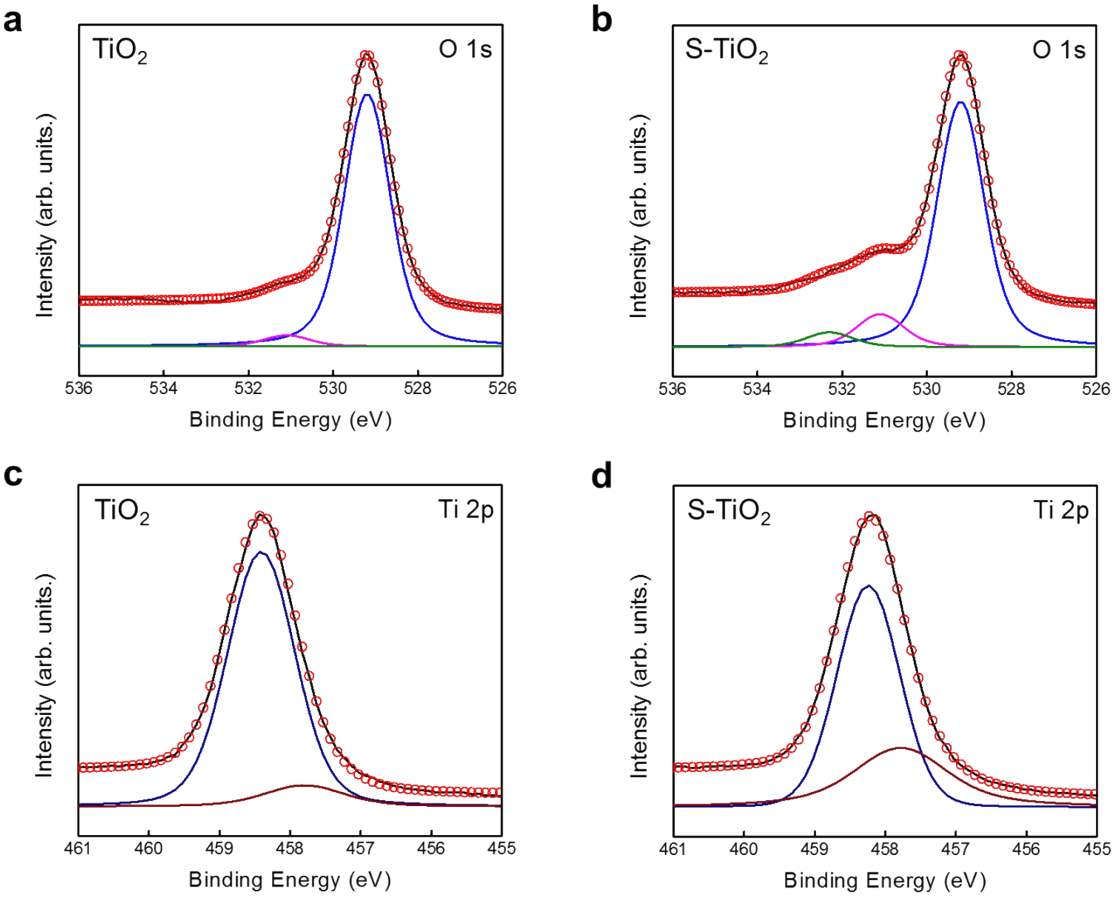

Figure S8. XPS analyses of TiO_2 and S-TiO_2. Right (Figure S8(a),(c)) TiO_2 data. Left (Figure S8(b),(d)) S-TiO_2 data. The O 1s peak was fitted by three peaks: those of the TiO_2 (Ti^{4+}) lattice in blue (529.3 eV), Ti_2O_3 (Ti^{3+}) in pink (531.1 eV), and TiO(C/H)Ti (absorption water) in green (532.3 eV). Also, the Ti 2p peak was fitted by two peaks: those of the TiO_2 (Ti^{4+}) lattice in navy (458.5 eV) and Ti_2O_3 (Ti^{3+}) in brown (457.8 eV).

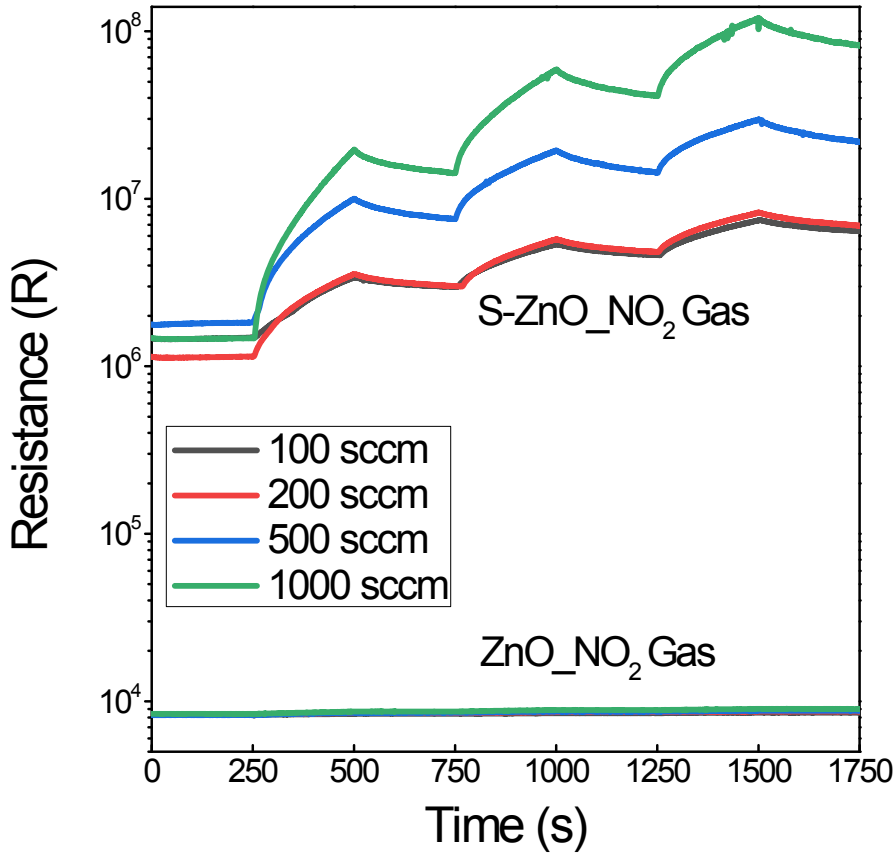

Figure S9. NO_2 gas reactivity data for ZnO and S-ZnO measured using the resistance value (R). Resistance data are shown on a log scale.

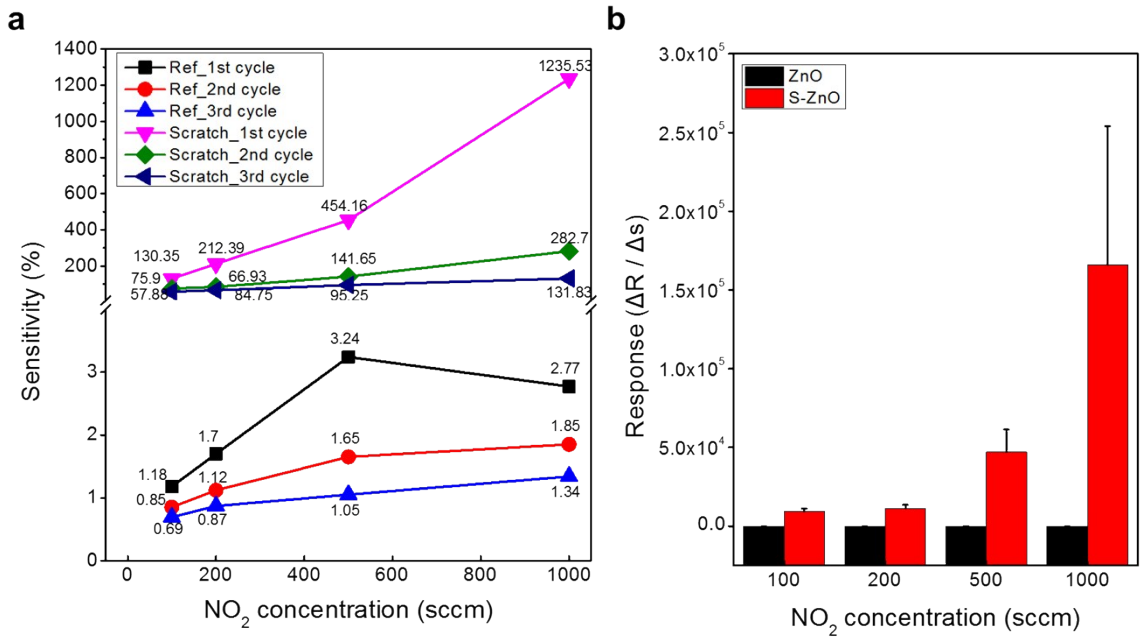

Figure S10. (a) The NO_2 gas sensitivities and (b) responses of the ZnO and S-ZnO samples. The sensor sensitivity and response of each sample was calculated by measuring them sequentially three times with the same NO_2 concentration (sccm). (Sensitivity (%): $(R_a-R_0)/R_a$ x 100, Response: $(R_a-R_0)/\Delta s$).

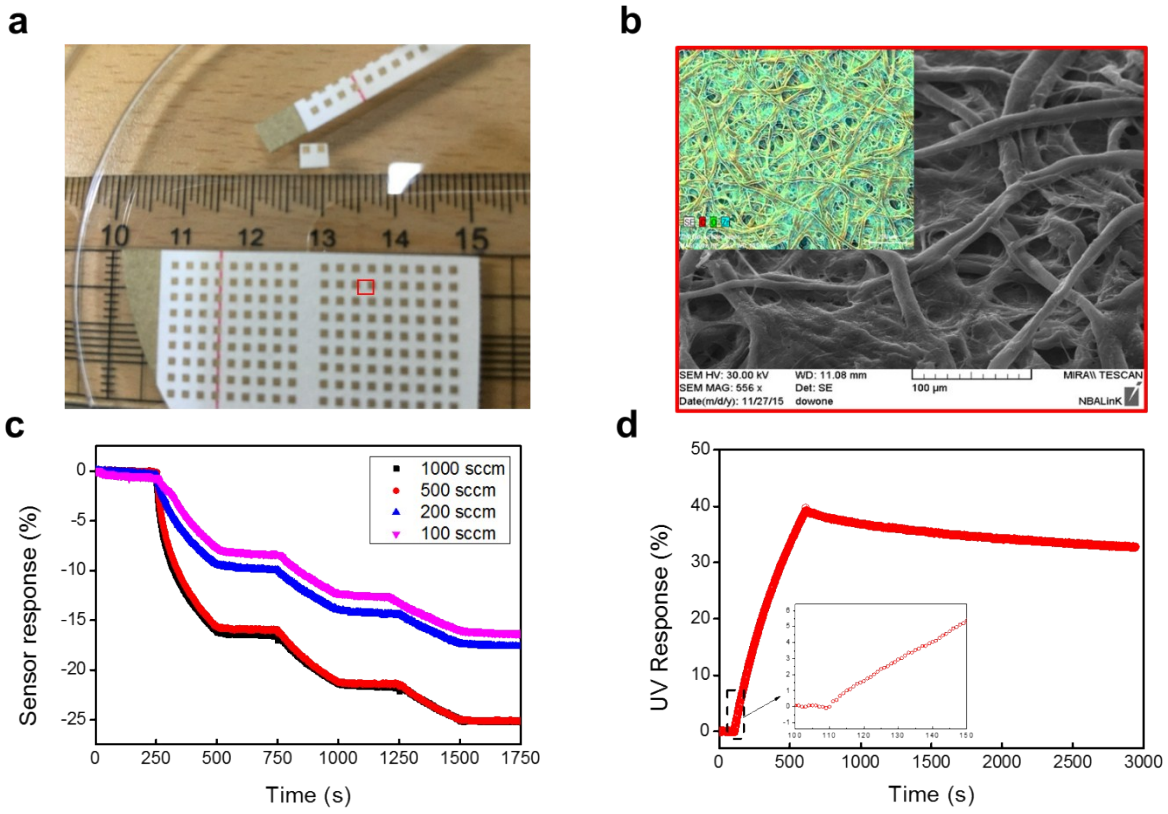

Figure S11. (a) Image of ZnO deposited using ALD on filter paper in order to maximize the effectiveness of the ZnO surface at sensing gas. A stencil mask was placed on the ZnO film and an Al electrode was deposited by thermal evaporation. The small red box in the photograph is the region analyzed with SEM in Figure S11b. (b) SEM image of ZnO on filter paper, and corresponding EDS map, which confirmed the presence of ZnO. (c) Responses of the gas sensor to NO_2 as a function of flow rate. (d) UV response data after the sensor response.

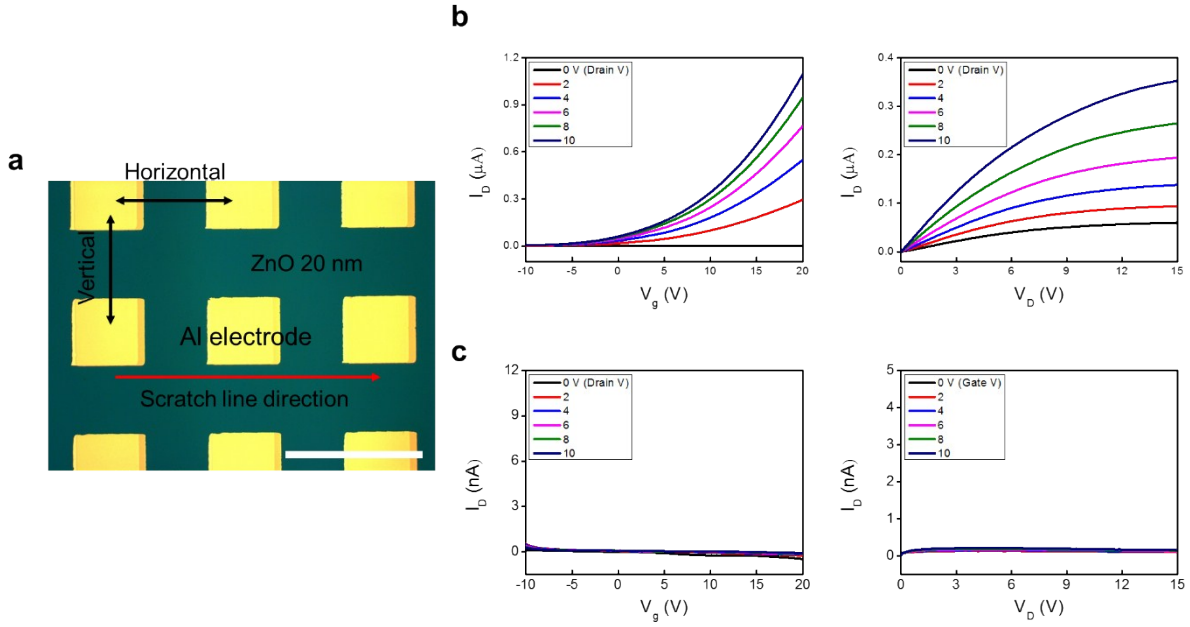

Figure S12. Electrical properties of S-ZnO fabricated with a 20 nm-thick ZnO film grown using ALD. (a) Optical microscope image of a device that shows the direction of the scratch. Scale bar; 1000 μm. (b) I-Vg (left) and I-V characteristics of S-ZnO measured parallel to the scratch direction. (c) I-Vg (left) and I-V characteristics of S-ZnO measured perpendicular to the scratch direction.

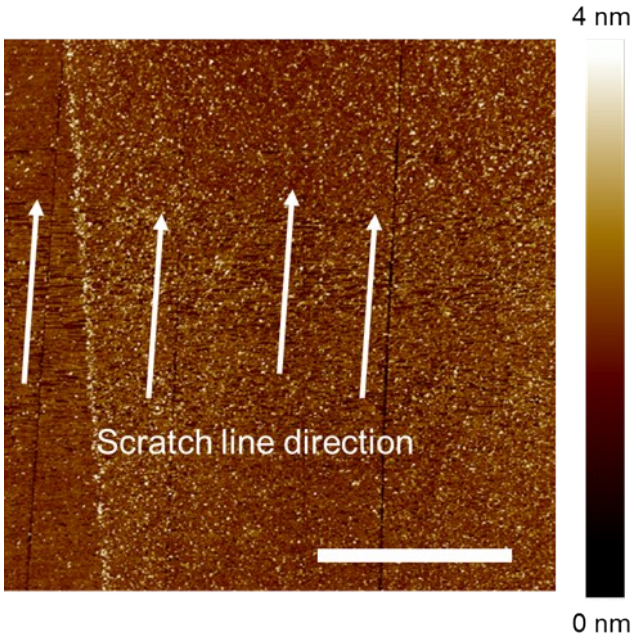

Figure S13. AFM image showing the scratches on SiO_2. ZnO (S-ZnO) on a SiO_2/Si substrate was rinsed with nitric acid (nitric acid (60%) : Di-W = 1 : 200) for 1 s to remove the S-ZnO layer. Scratched lines engraved on the SiO_2/Si substrate indicated that the use of scratch lithography effectively cut into the ZnO nanoribbons from the ZnO thin film. Scale bar: 3 μm.

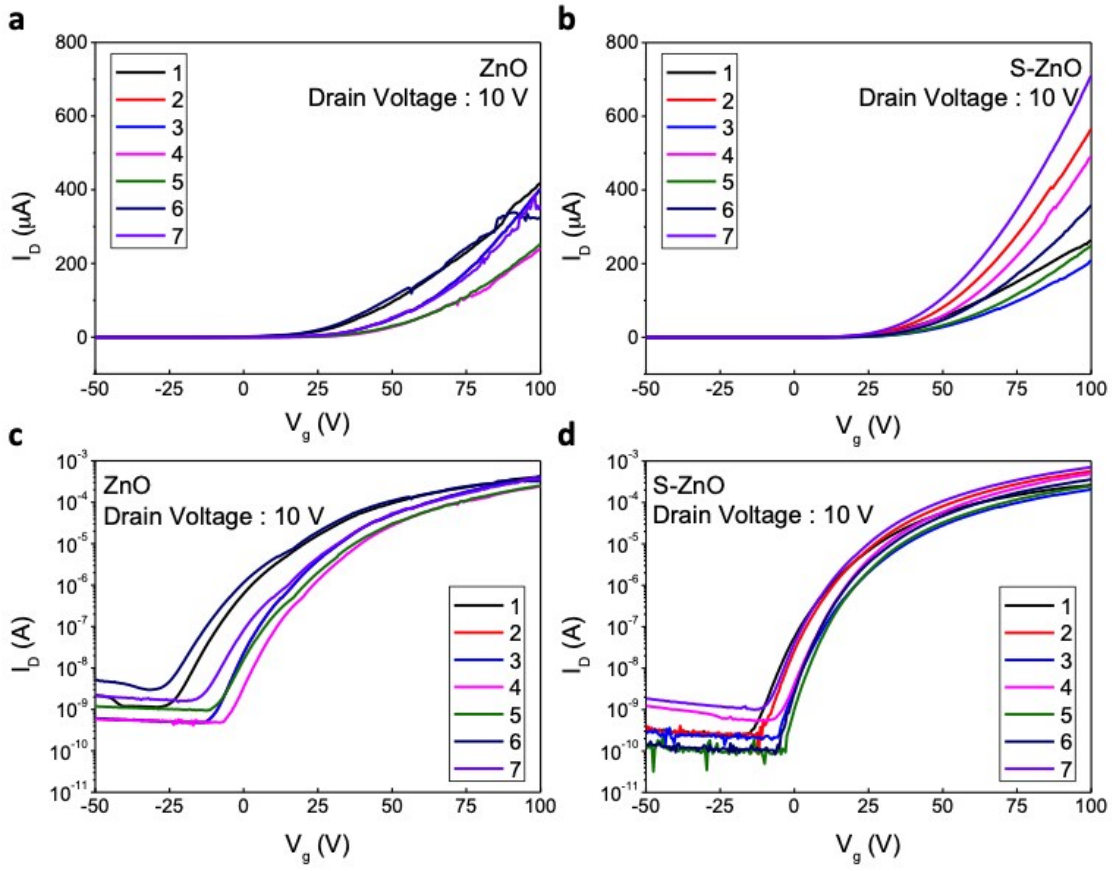

Figure S14. Electrical characteristics of semiconducting ZnO thin film and S-ZnO fabricated with semiconducting ZnO thin film. Transfer characteristics of ZnO and S-ZnO (semiconducting) were measured with 10 V (drain voltage). (a) and (b) show linear scale plot and (c),(d) log scale respectively, measured from 7 different samples of ZnO (semiconducting) and S- ZnO (semiconducting).

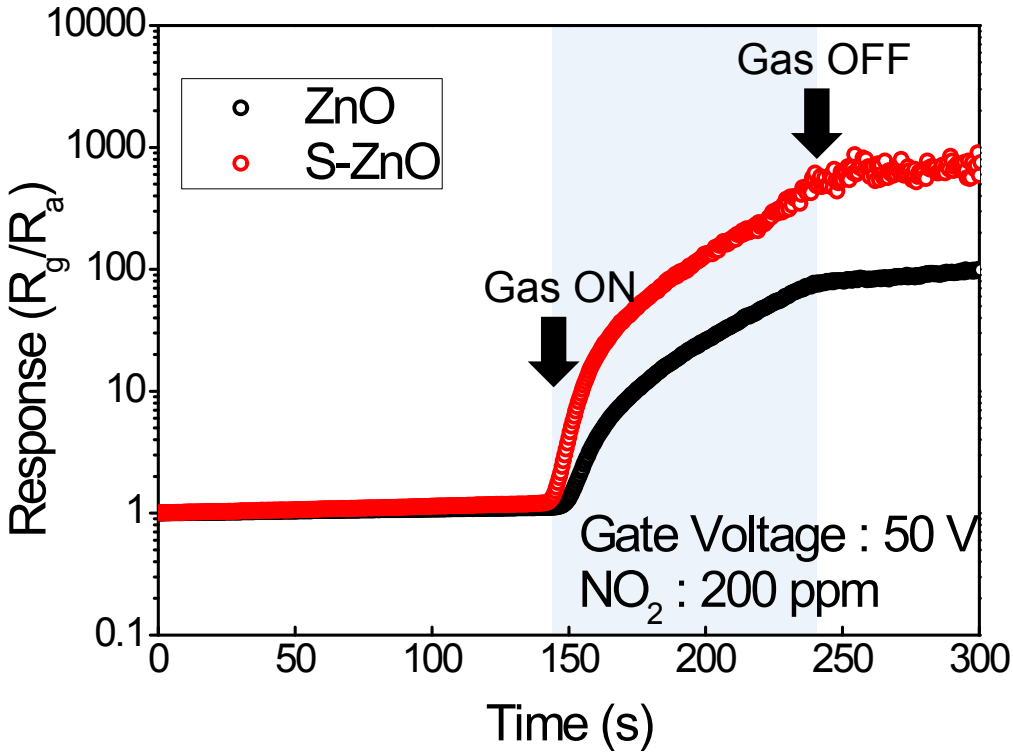

Figure S15. Sensor response comparison of semiconducting ZnO thin film (black) and S-ZnO (semiconducting) (red). Total flow rates of NO_2 and N_2 balancing gas were 500 sccm each at RT.

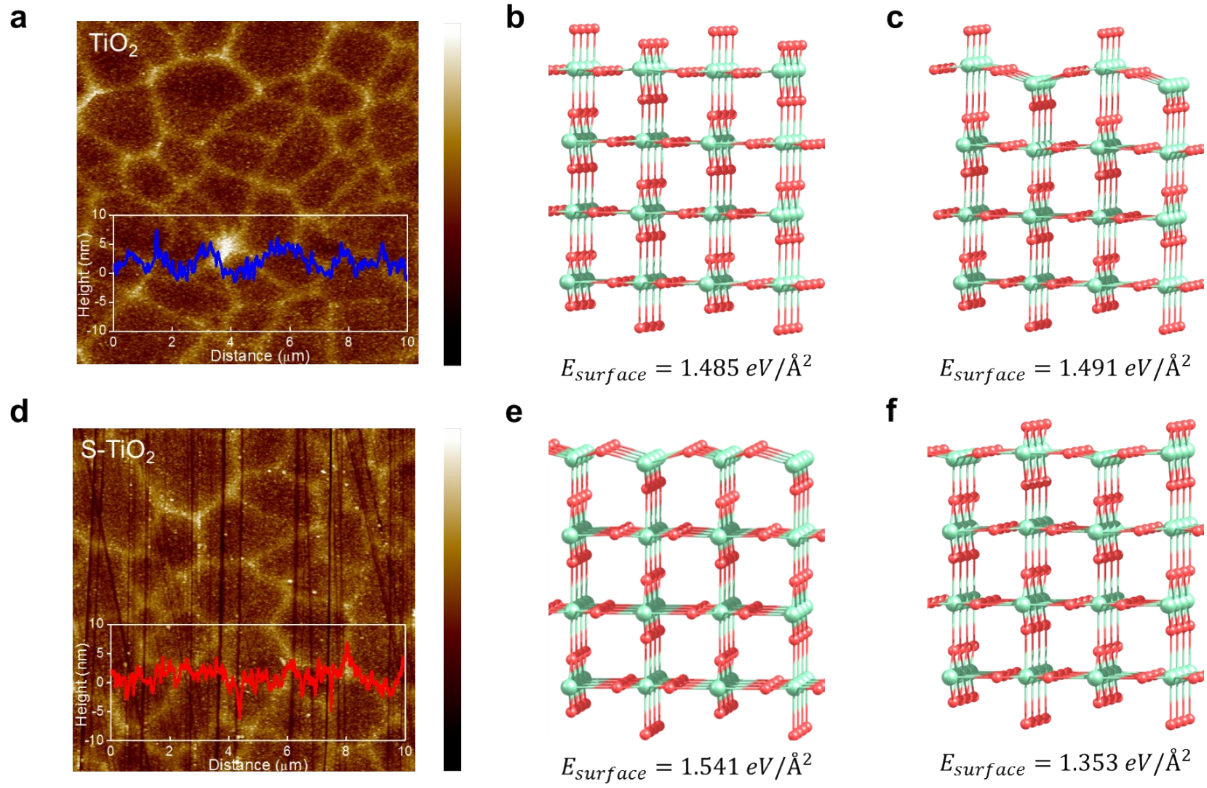

Figure S16. AFM images of (a) TiO_2 and (d) S-TiO_2 and atomic models of their surfaces. (b), (c), (e) and (f) Various surface configurations and surface energies of S-TiO_2(110); the geometry of the configuration shown in (f) was used for the calculations in **Table 1** since it was determined to have the lowest surface energy value.

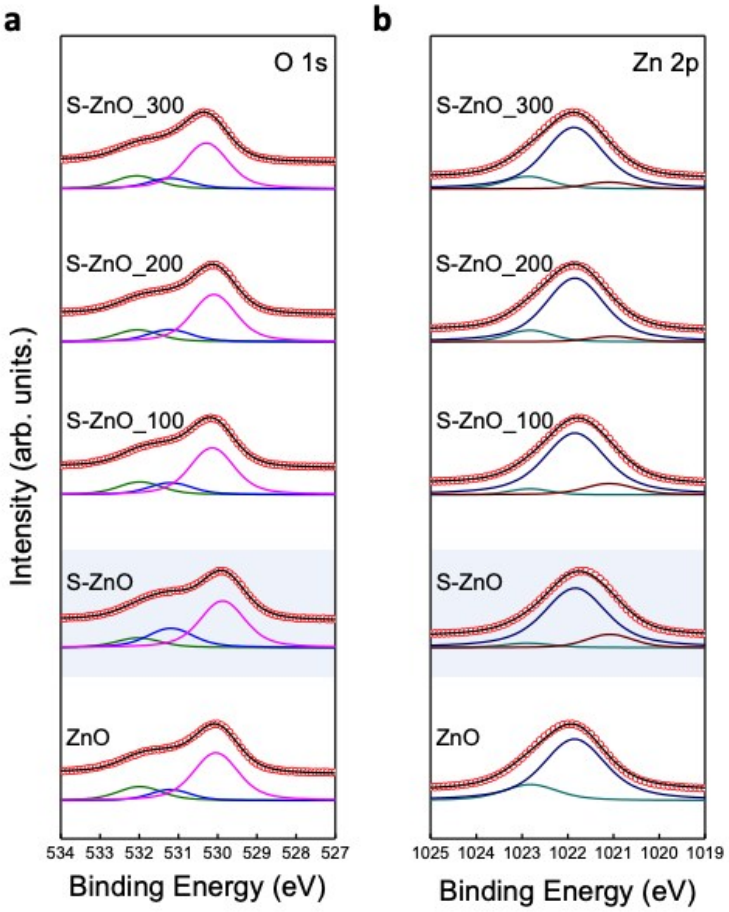

Figure S17. XPS spectra of S-ZnO before and after thermal annealing. (a), (b) represent O 1s and Zn 2p peak, respectively. After scratching, S-ZnO samples were heat-treated using a CVD (chemical vapor deposition) chamber at 100, 200 and 300 °C for 1 h in Air. Each O 1s peak was fitted by three peaks: those of the ZnO lattice in pink (529.9 eV), oxygen defect in green (531.4 eV), and hydroxyl groups of ZnO in blue (531.7 eV). Each Zn 2p peak was fitted by three peaks: those of zinc hydroxide in dark cyan (1022.8 eV), ZnO lattice in navy (1021.7 eV), and Zn metal in wine (1021.1 eV).

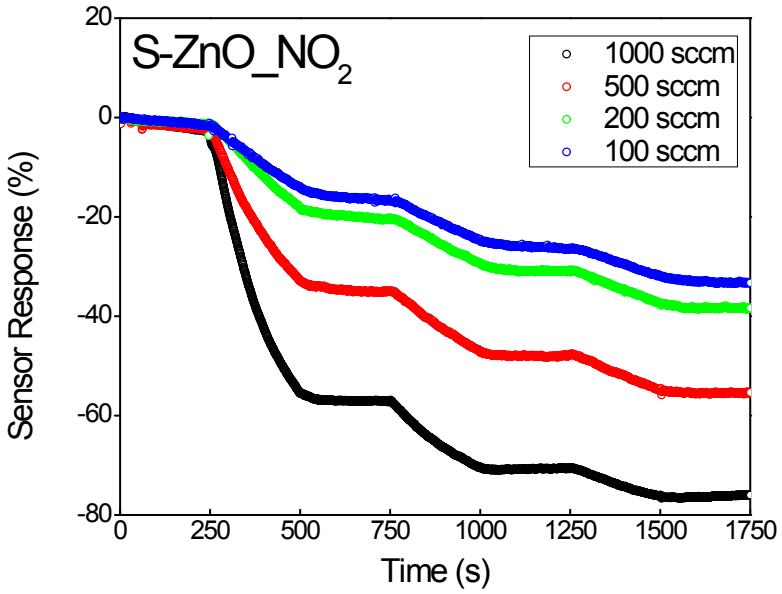

Figure S18. Long-term stability of a S-ZnO sensor device as indicated by measuring the sensor response after 2 months of shelf life.

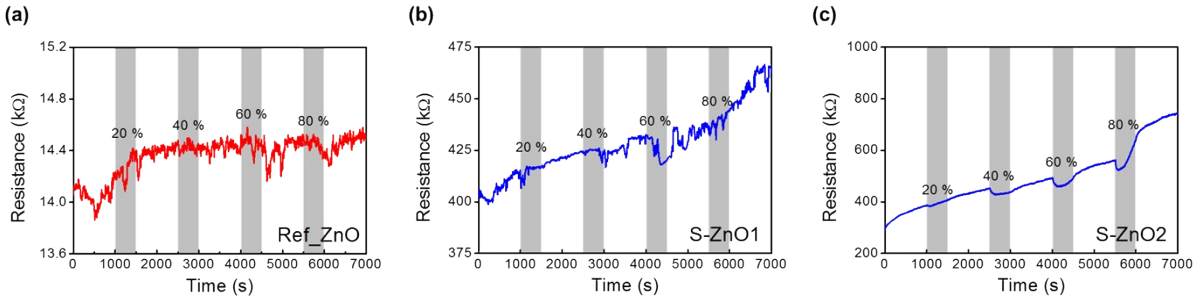

Figure S19. Humidity response properties. Time-dependent response sensing using ZnO (a) and S-ZnO (b-c) devices in different humidity (20-80 %) conditions. Total flow rate of N_2 balancing gas and H_2O bubbling gas is 500 sccm